

# Dynamics of p53 and Wnt cross talk.

Md.Zubair Malik<sup>1,3</sup>, Shah Nawaz Ali<sup>1,3</sup>, Md. Jahoor Alam<sup>2,3</sup>, Romana Ishrat<sup>1</sup>, R.K. Brojen Singh<sup>\*3</sup>

<sup>1</sup>Centre for Interdisciplinary Research in Basic Sciences, Jamia Millia Islamia, New Delhi-110025, India.

<sup>2</sup>College of Applied Medical Sciences, University of Hail, P.O. Box 2440, Hail, Kingdom of Saudi Arabia.

<sup>3</sup>School of Computational and Integrative Sciences, Jawaharlal Nehru University, New Delhi-110067, India

\* Corresponding author, E-mail: R.K. Brojen Singh - brojen@jnu.ac.in,

## Abstract

We present the mechanism of interaction of Wnt network module, which is responsible for periodic somitogenesis, with p53 regulatory network, which is one of the main regulators of various cellular functions, and switching of various oscillating states by investigating p53–Wnt model. The variation in Nutlin concentration in p53 regulating network drives the Wnt network module to different states, stabilized, damped and sustain oscillation states, and even to cycle arrest. Similarly, the change in Axin concentration in Wnt could able to modulate the p53 dynamics at these states. We then solve the set of coupled ordinary differential equations of the model using quasi steady state approximation. We, further, demonstrate the change of p53 and Gsk3 interaction rate, due to hypothetical catalytic reaction or external stimuli, can able to regulate the dynamics of the two network modules, and even can control their dynamics to protect the system from cycle arrest (apoptosis).

**Keywords:** p53 activation, Fixed point oscillations, Nutlin, Wnt, Sustain oscillations.

## Introduction

p53, one of the largest hub in cellular network [1, 2], is considered to be one of the most important key regulators of cellular metabolic pathways [3, 4], regulates a number of cellular functions [5] and its dynamics control even the fate of the cell when stress is given to the cell [6]. Further, p53 suppression is observed in various types of cancer either due to mutations or by ambiguous expression of control systems like MDM2 (or HDM2 its human equivalent) [7]. It is negatively regulated by the MDM2 [8], and functions as an E3 ligase which mediates the proteasomic degradation of p53 [9, 10], facilitates the diffusion of p53 in the nucleus [11], which in turn lowers the level of p53 within the cell [12]. In stressed cells, the p53 triggers the cell to cell cycle arrest forcing it to choose its fate, either to repair or apoptosis [13–15].

p53 dynamics is regulated by various signaling molecules as evident from various experimental and theoretical reports [16]. One of the most important inhibitor of p53–MDM2 is nutlin [17]. It is a selective small molecule which directly binds to binding pocket of MDM2 [18], to activate p53 pathway [18, 19], and inhibiting p53 binding to MDM2 [20]. Nutlin – 3a and 3b are the two most active enantiomorphs that are found to up-regulate the p53 in p53 dependent manner [21]. Further, it is also demonstrated that nutlin-3 induces anti-angiogenic activities in endothelial cells probably via three mechanisms; first by inhibiting endothelial cell migration; second by inducing cell cycle arrest; and third by increasing apoptotic tendency in endothelial cells [22]. Further, it was also shown that nutlin-3 treatment in these cells leads to accumulation of p53 [23], indicating the important impacts of nutlin-3 which interferes the p53–MDM2 regulatory mechanism. As a consequence, it was shown that Nutlin-3 stabilizes the p53 dynamics and causes the activation of survival pathways [23].

Somitogenesis in vertebrates is periodic formation of somites (vertebrae precursors) in the anterior presomitic mesoderm tissue (PSM) controlled by complex gene network known as segmentation clock [24],

where, Notch, Wnt pathways [25, 26] and fibroblast growth factor (FGF) are the main components [27]. Further, it has been shown that these three main pathways generate rhythms of specific oscillation relationships [27], and cross-talk among them [28] as a basis of spatio-temporal self-organization of patterns during somitogenesis [29]. This physiological oscillations is responsible for periodic spacing of somites, dynamic structures and regular segmented development in vertebrates [29]. In some studies in normal (stress) and cancerous cells, it has been reported that *p53* and Wnt modules are being coupled and cross-talk between them via different intermediate proteins or genes or signaling molecules [30–32]. The studies also reported that *p53* network suppresses the Wnt signaling cascade [31]. The Wnt signaling plays a pivotal role in determination of cell fate, which may probably through *p53* interaction [31, 32], but still it is not clear yet. Further, several other works reported that the intercellular signaling of Wnt depends on the  $\beta$ -catenin and glycogen synthase kinase-3 (*GSK-3*) [33]. Moreover, *p53* can regulate the dynamics of *Axin2* and *GSK-3* [34]. Recently, it is also reported that the *miR* – 34 family, which is directly transcribed by the *p53*, links *p53* with Wnt signaling [32], in this process, and a set of *GSK-3*-related Wnt genes, are directly targeted by *p53* and *miR*-34. These observations clearly suggest the close connection between the *p53* functionalities and Wnt in stress and cancer cells [30, 32]. However, the way how *p53* interacts with Wnt during somitogenesis and its impact on somite organization/reorganization at molecular level is still an open question.

*GSK-3*, which is an important coupling molecule between *p53* and Wnt pathways, is widely expressed in broad range of cellular processes and being a Ser/Thr kinase it is a multifunctional protein [35, 36]. It is active under resting condition and act as a core regulator in various disease pathways like cancer [35]. Being a kinase, it confers selectivity and substrate specificity [35]. It also largely acts as a phosphorylating and an important signaling agent for the degradation of large number of proteins, such as  $\beta$ -catenin in Wnt pathway [37]. Further, it is a central player in Wnt signaling pathway recruited with the *Axin2* at the Frizzles receptor for the activation of Wnt signaling [38]. In absence of Wnt signals *GSK-3* shows its activity in the protein destruction complex with *Axin2*, APC (adenomatous polyposis coli) and other partners mediating the destruction and phosphorylation of  $\beta$ -catenin [39]. *GSK-3* also mediates *p53* dependent apoptosis signaling by suppressing *p53*-AKT pathway. The role *GSK-3* as a mediator of *p53* and Wnt cross-talk is not fully understood. The impact of other Wnt regulators in Wnt pathway and how they regulate *p53* dynamics, and vice versa, are needed to be investigated in order to understand how segmentation clock works.

We study the coupling of Wnt oscillator which is one of the three important clocks in somitogenesis in vertebrates and *p53* regulatory network to understand how does these two oscillators regulates each other and process information during somite formation and pattern organization. Since *p53* interferes various other cellular functions, it will be interesting to understand its regulating impacts on segmentation clock and vice versa. Presently we study these phenomena by modeling this *p53*-Wnt two oscillator model with updated interaction between them from various experimental reports and how do they regulate each other. We organize our work as follows. The detailed description of the model and techniques is provided in materials and methods section. It is followed by mathematical treatment of the model, the numerical simulation results and its discussion in the next section. We then draw some conclusions based on the results we obtained and discussion on it.

## Materials and Methods

### A. Coupling *p53*-Wnt Oscillators Model

The Wnt signaling pathway is authorized by  $\beta$ -catenin regulation via various intermediate interaction steps (Fig. 1) [40, 41]. In this signal processing, Wnt promotes the synthesis of Dishevelled (Dsh) protein, and then inhibits *GSK3* protein kinase [27]. *GSK3*, then interacts with *Axin* (with rates  $k_1$  and  $k_2$  for forward and backward reactions as in Fig.1) in the presence of  $\beta$ -catenin to form transient complex which

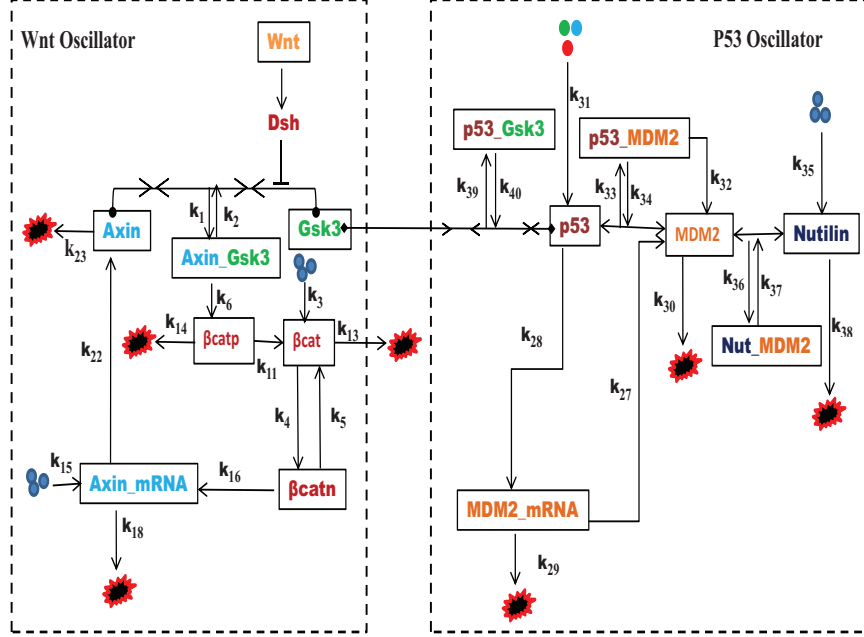


**Figure 1.** The schematic diagram of biochemical network of *p53* and Wnt modules and their cross talk via GSK3.

in turn phosphorylates  $\beta$ -catenin into  $\beta$ -catenin-P (with rate  $k_6$ ) [27, 41]. The  $\beta$ -catenin-P degraded quickly with rate  $k_{14}$ , on the other hand it is dephosphorylated with rate  $k_3$  to form freed  $\beta$ -catenin and then degraded with a rate  $k_{13}$  [42]. The free  $\beta$ -catenin is then transported to nucleus ( $\beta$ -catenin-n) with rate  $k_4$ , on the other hand  $\beta$ -catenin-n is transported from nucleus to cytoplasm with another rate  $k_5$ . Then  $\beta$ -catenin-n promotes the transcription of set of target genes including mAxin (mRNA of Axin, specifically homolog Axin2 in PSM tissue) at the rate  $k_{15}$ , with rate  $k_{16}$ , and mAxin also degrades with a rate  $k_{18}$  [43]. On the other hand mAxin translates to Axin with a rate  $k_{18}$ . Axin protein which also degrades with a rate  $k_{23}$ . This mechanism of Axin is just like a negative feedback loop which drives the oscillations in the network components. Thus *Axin2* is the essential target of the Wnt pathway because it inhibits the Wnt signals by degrading the  $\beta$ -catenin by forming a negative feedback loop [44].

The Wnt pathway communicates with the *p53* Oscillator [45–47] through *GSK3* by formation of a binary complex *p53* – *GSK3* with the free available *p53* at the rate  $k_{39}$ . Then this complex *p53* – *GSK3* degrades at the rate  $k_{40}$  to the free *p53* and *GSK3* proteins [48]. *p53* and *MDM2* regulate each other

with feedback mechanism where formation and decay of various intermediate complexes are involved with different rates (Fig. 1) as described in Table 1 and 2 [45]. The freely synthesized Nutlin directly interacts with *MDM2* with a rate  $k_{36}$  to form a complex  $Nut_MMDM2$ , and then this complex dissociates to release back free Nutlin and *MDM2*. Then Nutlin indirectly interacts with *p53* via *MDM2* by affecting the feedback mechanism between *p53* and *MDM2*. The Nutlin then degrades with rate constant  $k_{38}$ . Thus the activated *p53* can now go to the nucleus and initiate the transcription of a number of target genes including *MDM2*. *MDM2* is essential in controlling the concentration of *p53* through a positive feedback loop mechanism by making complex [49, 50].

### Mathematical model of the network: Quasi steady state approximation

The stress *p53* – *Wnt* regulating network we study is defined by  $N = 13$  molecular species (Table 1) corresponding to the reaction network description provided in Table 2. The state of the system at any instant of time  $t$  is given by the state vector,  $\vec{x}(t) = (x_1, x_2, \dots, x_N)^T$ , where,  $N = 13$  and  $T$  is the transpose of the vector. By considering feedback mechanism of in *p53* and *Wnt* oscillators and coupling reaction channels of the two oscillators, we could able to reach the following coupled ordinary differential equations (ODE),

$$\frac{d}{dt}\vec{x}(t) = \begin{bmatrix} F_1 \\ F_2 \\ \vdots \\ F_{13} \end{bmatrix} \quad (1)$$

where, the functions in the equation (1)  $\{F_i(x_1, x_2, \dots, x_N)\}$ ,  $i = 1, 2, \dots, 13$  are given by,

$$F_1 = k_{26} \left[ k_{22}x_2 - k_{23} \frac{x_1}{k_{24} + x_1} - k_1x_1x_6 + k_2(k_8 - x_6) \right] \quad (2)$$

$$F_2 = k_{26} \left[ k_{15} + k_{16} \frac{(x_5)^{k_{25}}}{(k_{17})^{k_{25}} + (x_5)^{k_{25}}} - k_{18} \left( \frac{x_2}{k_{19} + x_2} \right) \right] \quad (3)$$

$$F_3 = k_{26} \left[ k_3 - k_6 \left( \frac{k_9}{k_9 + k_7} \right) \left( \frac{x_3}{k_{10} + x_3} \right) \left( \frac{k_8 - x_6}{k_8} \right) + k_{11} \left( \frac{x_4}{k_{12} + x_4} \right) \right] - k_{26} [k_4x_3 - k_5x_5 + k_{13}x_3] \quad (4)$$

$$F_4 = k_{26} \left[ k_6 \left( \frac{k_9}{k_9 + k_7} \right) \left( \frac{x_3}{k_{10} + x_3} \right) \left( \frac{k_8 - x_6}{k_8} \right) - k_{11} \left( \frac{x_4}{k_{12} + x_4} \right) - k_{14}x_4 \right] \quad (5)$$

$$F_5 = k_{26} [k_4x_3 - k_5x_5] \quad (6)$$

$$F_6 = k_{26} (-k_1x_1x_6 + k_2k_8 - k_2x_6) - (k_{39}x_7x_6 + k_{40}x_{13}) \quad (7)$$

$$F_7 = k_{31} - k_{33}x_7x_8 + k_{34}x_{10} - k_{39}x_7x_6 + k_{40}x_{13} \quad (8)$$

$$F_8 = k_{27}x_9 - k_{30}x_8 + k_{32}x_{10} - k_{33}x_7x_8 + k_{34}x_{10} - k_{36}x_{11}x_8 \quad (9)$$

$$F_9 = k_{28}x_7 - k_{29}x_9 + k_{41}x_{13} \quad (10)$$

$$F_{10} = -k_{32}x_{10} + k_{33}x_7x_8 - k_{34}x_{10} \quad (11)$$

$$F_{11} = k_{35} - k_{36}x_{11}x_8 + k_{37}x_{12} - k_{38}x_{11} \quad (12)$$

$$F_{12} = k_{36}x_{11}x_8 - k_{37}x_{12} \quad (13)$$

$$F_{13} = k_{39}x_7x_6 - k_{40}x_{13} \quad (14)$$

The coupled ODEs (equation (1)) are very difficult to solve analytically. However, one can get approximate analytical solution of these equations by using quasi-steady state approximation [51, 52]. In

general, any biochemical reactions network involves two basic types of reaction, namely slow and fast reactions [51]. Therefore, the  $N = 13$  variables in the system can be divided into sets of slow and fast variables respectively. If  $\vec{x}^s(t) = (x_1, x_2, \dots, x_l)^T$  and  $\vec{x}^f(t) = (x_{l+1}, x_{l+2}, \dots, x_N)^T$  are slow and fast variable vectors, then  $\vec{x}(t) = (\vec{x}^s, \vec{x}^f)^T$ . Then from equation (1)-(14) along with Table I, we have,

$$\vec{x}^s(t) = \begin{bmatrix} x_1 \\ x_3 \\ x_6 \\ x_7 \\ x_8 \\ x_{11} \end{bmatrix}; \quad \vec{x}^f(t) = \begin{bmatrix} x_2 \\ x_4 \\ x_5 \\ x_9 \\ x_{10} \\ x_{12} \\ x_{13} \end{bmatrix} \quad (15)$$

Since the rate of complex formation is fast, and after this fast complex formation, the fast variables immediately retain steady state (equilibrium). Then using Henri-Michaelis-Menten-Briggs-Haldane approximation [53], one can take quite fair assumption that the ODEs of variables of complex molecular species reach steady state equilibrium quite fast compared with the time evolution of slow variables [51]. Then one can straight forward put,  $\frac{d\vec{x}^f}{dt} \approx 0$  [51, 53]. Now, the number of coupled ODE (1) reduces to the following,

$$\frac{d\vec{x}(t)}{dt} = \frac{d\vec{x}^s(t)}{dt} = \frac{d}{dt} \begin{bmatrix} x_1 \\ x_3 \\ x_6 \\ x_7 \\ x_8 \\ x_{11} \end{bmatrix} \quad (16)$$

and the  $\vec{x}^f$  become the following steady state values,

$$\vec{x}^s \rightarrow \begin{bmatrix} x_2^* \\ x_4^* \\ x_5^* \\ x_9^* \\ x_{10}^* \\ x_{12}^* \\ x_{13}^* \end{bmatrix} \rightarrow \text{constant} \quad (17)$$

The thirteen ordinary differential equations are now reduced to six ordinary differential equations. This allows to simplify the complex mathematical model to get approximate solutions of the system numerically saving computational cost or analytically from the reduced system if possible.

We used standard Runge-Kutta method (order 4) of numerical integration to simulate equation (re-fode) to find the solution of the variables listed in Table 1 for the parameter values given in Table 2. We then analysed the constructed mathematical model to get possible approximate analytical solutions of the variables (slow variables) using quasi-steady state approximation.

## Results and Discussion

The cross talk between p53 and Wnt via Gsk3 subjected to different stress conditions induced by nutlin, as well as Axin concentrations available in the system. In order to understand how they regulate each other, we numerically simulated the coupled ordinary differential equations (1) with the parameters listed

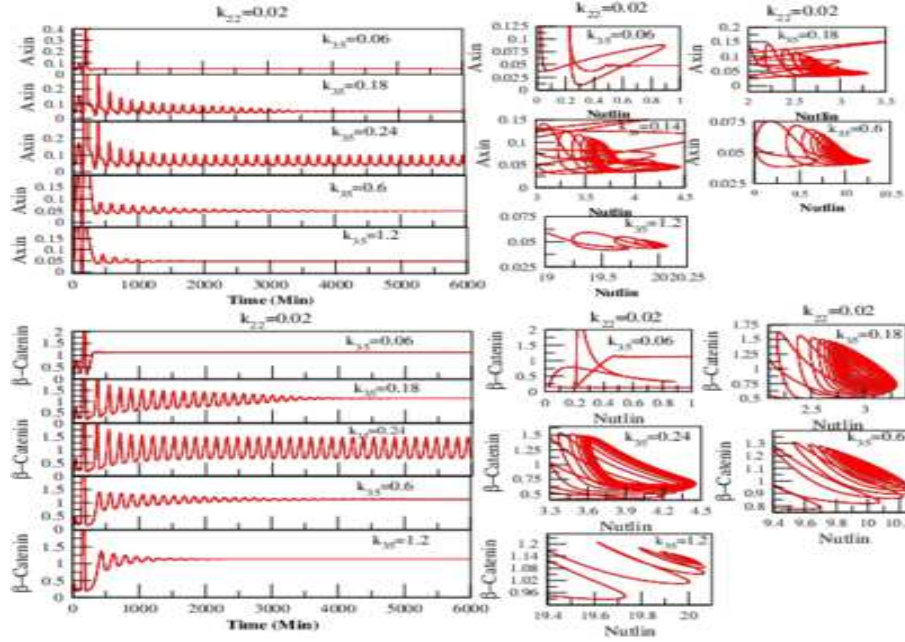


**Figure 2.** The dynamics of Axin and  $\beta$ -catenin for different values of  $k_{35}$  i.e. 0.06, 0.18, 0.24, 0.6 and 1.2 for fixed value of  $k_{22} = 0.02$ . The right hand panels are the two dimensional plots the Axin and  $\beta$ -catenin with nutlin for the same set of parameter values showing different state behaviors.

in Table 2. The simulation results for the variable in the model are presented and compared to understand the switching of different oscillating states induced by different stress conditions. The reason is that these states of the oscillations in Wnt network are responsible for different behavior of regular somite formation, and many other periodic phenomena during somitogenesis. The roles of *Axin2*, *Gsk3*,  $\beta$ -catenin and Nutlin on the *p53* network dynamics is discussed in the context of the model we presented. Further, the signal processing between the two coupled network modules via the *Gsk3* during somitogenesis is studied under the stress *p53* generating effect due to *Nutlin-3a*. On the other hand, we also studied the regulation of *p53* by Wnt due to available Axin concentration in the system.

### Driving Wnt oscillating states by *p53*

The *p53* in *p53* regulatory network can be induced stress by the available concentration of stress inducer molecular species, *Nutlin-3a*. The concentration level of *Nutlin-3a* is proportional to the creation rate constant of *Nutlin-3a*,  $k_{35}$  (Fig. 1). Therefore, computationally we can able to monitor the amount of stress induced to *p53* by changing the value of parameter  $k_{35}$  and supervising the dynamical behavior of *p53* (Fig. 2 and 3).

The dynamics of *p53* (Fig. 2 upper left panels) for small values of  $k_{35}$  ( $k_{35} < 0.07$ ) show single spike due to sudden stress, and due to small  $k_{35}$  values, the dynamics become stabilized indicating normal nature of the system. Then, as the value of  $k_{35}$  increases, *p53* dynamics show damped oscillation indicating the inducing oscillation for certain interval of time ( $t \approx [0, 4000]$  minutes for  $k_{35} = 0.18$ ), and then its dynamics become stabilized. The time interval of damped oscillation regime depends on the value of  $k_{35}$  and increases as  $k_{35}$ . This indicates that if the stress given to the system is small, the system first will go to the stress or excited state (indicated by oscillatory behavior), repair back the changes in the system



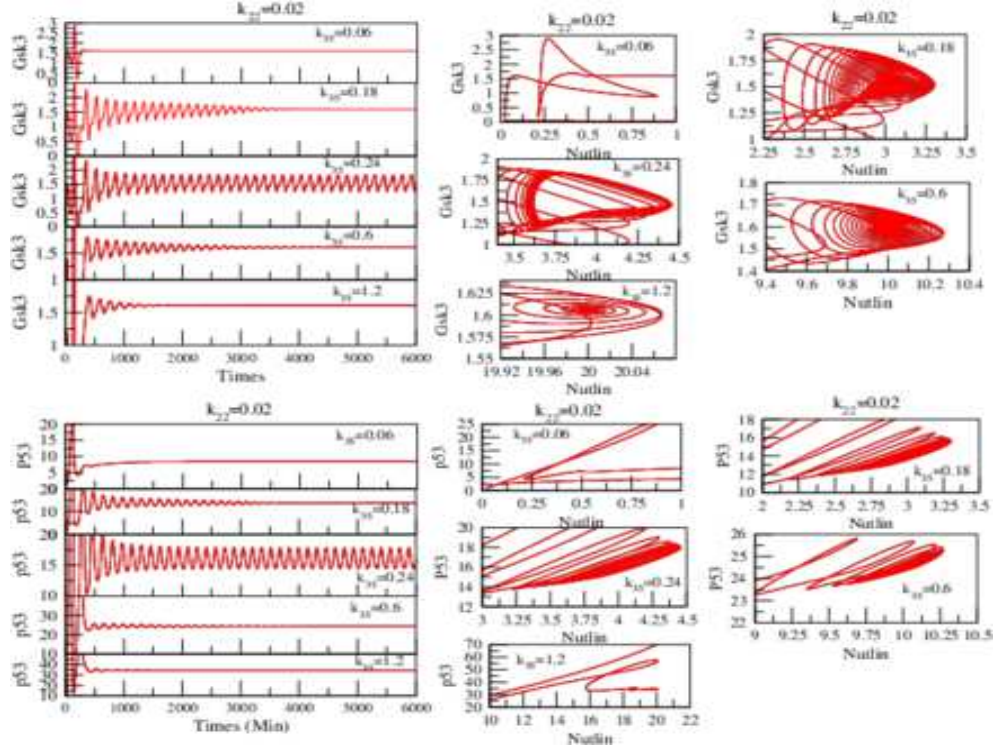


**Figure 3.** The similar plots for  $p53$  and  $Gsk3$  for the same set of values as in Figure 2.

and come back to the normal condition. For sufficiently large values of  $k_{35}$  ( $0.23 \leq k_{35} \leq 0.55$ ) the  $p53$  dynamics become sustain oscillation, where the responded stress is optimal and sustains the stress for  $t \rightarrow \infty$ . Further increase in the value of  $k_{35}$  ( $k_{35} > 0.55$ ) force the sustain oscillation of  $p53$  to damped oscillation whose time interval of damped oscillation decreases as  $k_{35}$  increases. This indicates that excess stress in  $p53$  due to Nutlin may become toxic to the system reflected in  $p53$  dynamics. If we increase the value of  $k_{35}$  ( $k_{35} > 1.3$ ) the  $p53$  dynamics become stabilized. This may probably the case of apoptosis of the system. The results obtained are in consistent with the experimental observations which indicates that acetylation of  $p53$  is responsible for its activation and stabilization [54]. If we further increase the value of  $k_{35}$ ,  $p53$  activation decreases maintaining  $p53$  stability, but at higher values ( $\leq 35$ ).

The two dimensional plots between  $p53$  and Nutlin (Fig. 2 upper right panels) for different values of  $k_{35}$  show different behaviors of the system, namely stable fixed point, damped oscillation towards a fixed point, sustain oscillation, then damped and stabilized fixed point. This behaviors show the same behaviors as shown in  $p53$  dynamics for different values of  $k_{35}$ .

Similarly, we study the dynamics of  $Gsk3$  as a function of  $k_{35}$  (Fig. 2 lower left panels) for corresponding values which we took for the case of  $p53$ . In this case also we found the similar behaviors as we got in  $p53$  case (Fig. 2), namely, stabilized, damped, sustain, then damped and stabilized states for the corresponding values of  $k_{35}$  taken in  $p53$  case. The two dimensional plots of  $Gsk3$  and Nutlin (Fig. 2 lower right hand panels) show the evidence of the existence of the mentioned states.

Now we study the dynamics of Axin (Fig. 3 upper left panel) imparted by stress  $p53$  via  $Gsk3$  induced by Nutlin concentration in the system. The signal of the stress  $p53$  is processed by Axin via  $Gsk3$  and reflected the same states in Axin dynamics as obtained in  $p53$ . The Axin and  $\beta$  - *Catenin* dynamics as a function of  $k_{35}$ , as well as two dimensional plots of these two molecules with Nutlin are similar

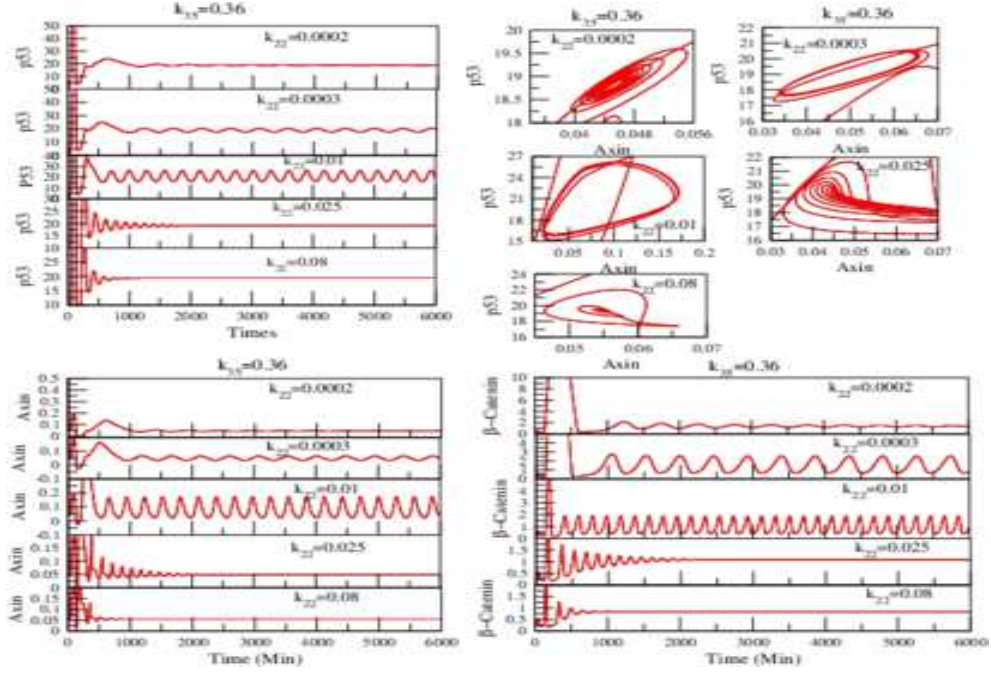


**Figure 4.** Plots of  $p53$ , Axin and  $\beta$ -catenin as a function of time for  $k_{22}$  values 0.0002, 0.0003, 0.01, 0.025 and 0.08, for fixed values of  $k_{35}$ . The upper right panels shows the two dimensional plots of  $p53$  and  $\beta$ -catenin with Axin for same set of  $k_{22}$  and  $k_{35}$  parameter values.

qualitatively with the dynamics of stress  $p53$  and  $Gsk3$  (Fig. 2 and 3). This means that depending on the values of  $k_{35}$  the stress  $p53$  can able to generate and arrest the Axin and  $\beta$ -Catenin cycles. Thus the dynamics of Axin and  $\beta$ -Catenin can be regulated by  $p53$  and probably can control the Wnt oscillator. This means that  $p53$  regulation has strong impact on Wnt oscillation, and regulate various mechanisms during sometogenesis.

### Dynamics of $p53$ regulated by Wnt

The activation of Axin occurs after the  $Gsk$  initiation from the signal received at the membrane. The Nutlin synthesis rate ( $k_{35}$ ) is kept constant in this case ( $k_{35} = 0.36$ ), giving a slight stress to the system. In order to understand how does Wnt oscillator regulate  $p53$ , we allow to change Axin synthesis rate  $k_{22}$  and see the dynamical behavior of  $p53$  induced by Axin, which is one of the most important molecular species in Wnt network module. The dynamics of the Axin and  $p53$  for different values of  $k_{22}$  (Fig. 4). For small values of  $k_{22}$  ( $k_{22} < 0.0002$ ), Axin dynamics maintains lowest constant level, showing stabilized state of the Axin dynamics (Fig. 4 lower left panels). The increase in the value of  $k_{22}$  allows the Axin dynamics to switch from stabilized state to damped state for certain range of time and then become stabilized. The co-existence of these two states (damped and stabilized states) takes place for a certain range on  $k_{22}$  ( $0.0003 < k_{22} < 0.008$ ). If we increase the value of  $k_{22}$ , the duration of damped oscillation also increases. The switching of damped state to sustain oscillation state takes place for certain range of  $k_{22}$ ,  $0.0087 < k_{22} < 0.015$ . Further increase in  $k_{22}$  force the sustain oscillation state to damped oscillation state again, where the time interval of damped oscillation becomes smaller as  $k_{22}$  increases. If we increase  $k_{22}$  value, then Axin dynamics landed to stabilized state.



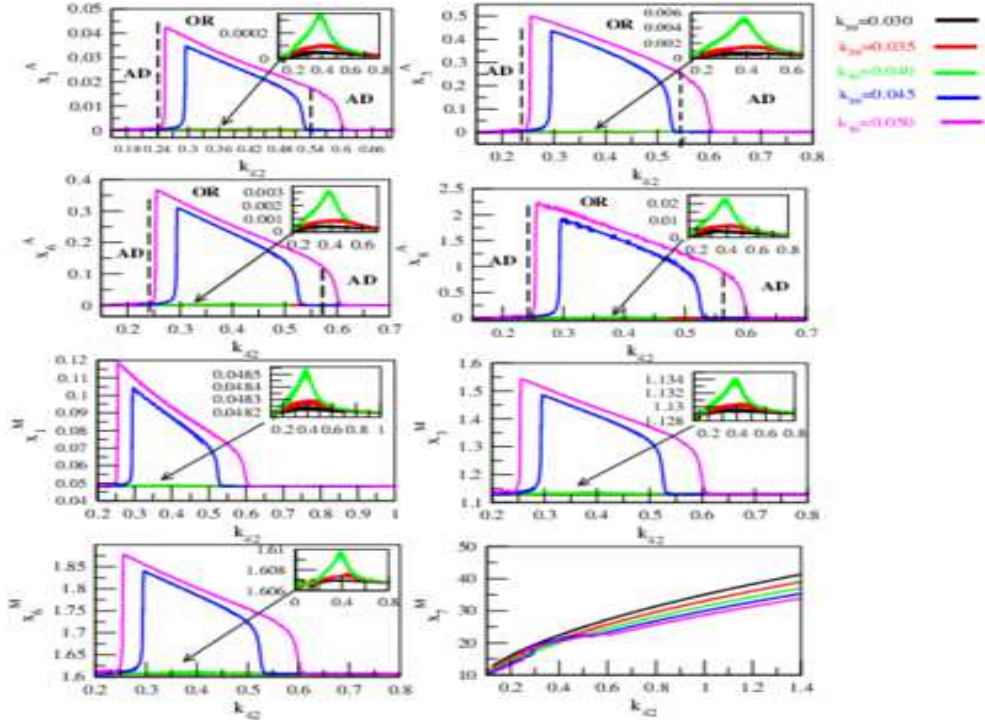


**Figure 5.** The amplitudes of  $p53$  ( $x_1^A$ ),  $\beta$ -catenin ( $x_3^A$ ),  $Gsk3$  ( $x_6^A$ ) and  $Mdm2$  ( $x_8^A$ ) as a function of  $k_{35}$  for various  $k_{39}$  values 0.030, 0.035, 0.040, 0.045 and 0.050 (upper four panels). The lower four panels are the maxima of  $p53$  ( $x_1^M$ ),  $\beta$ -catenin ( $x_3^M$ ),  $Gsk3$  ( $x_6^M$ ) and  $p53$  ( $x_7^M$ ) for the set of parameter values.

We then show the dynamics of  $\beta$ -Catenin as a function of  $k_{22}$  (Fig. 4) which indicates the switching of the three different states driven by  $k_{22}$ . In this case we could able to find sustain oscillation very quickly indicating that the  $\beta$ -Catenin can be quickly switch to stress condition and easily. Similarly,  $\beta$ -Catenin can reach second stabilized state (probably cycle arrest) quickly and easily as compared to other molecular species. The dynamical behavior of  $\beta$ -Catenin is supported by two dimensional plots of  $\beta$ -Catenin and Axin (Fig. 3 middle right panels) which exhibit fixed point oscillations (corresponding to two stabilized states), attractor towards the stable fixed points (corresponding to two damped oscillations), limit cycle (corresponding to sustain oscillation).

Now the dynamics of  $p53$  as a function of  $k_{22}$  (Fig. 4 upper left panel) show that the patterns in the dynamics of molecular species in Wnt oscillator are well captured in the  $p53$  dynamics. The  $p53$  dynamics exhibit the corresponding states, namely, stabilized, damped and sustain oscillation states, as observed in Axin and  $\beta$ -Catenin as a function of  $k_{22}$  with similar patterns and dynamics.

The important dynamical behaviors those have been captured in  $p53$  dynamics due to change of states in molecular species in Wnt oscillator are synchronous in states and time periods of dynamics. If we look at the dynamics of Axin and  $\beta$ -Catenin as a function of  $k_{22}$ , we can easily observe two important changes, (1) change in time period of oscillations of the molecular species, and (2) change in the pattern of states. The increase in  $k_{22}$  force to decrease the time period of the Axin and  $\beta$ -Catenin dynamics. At the same time the switching of the various states takes place. These changes in the Axin and  $\beta$ -Catenin are systematically and synchronously well captured in qualitative sense in the  $p53$  dynamics (Fig. 4) during the communication of the two  $p53$  and Wnt oscillators via  $Gsk3$ .

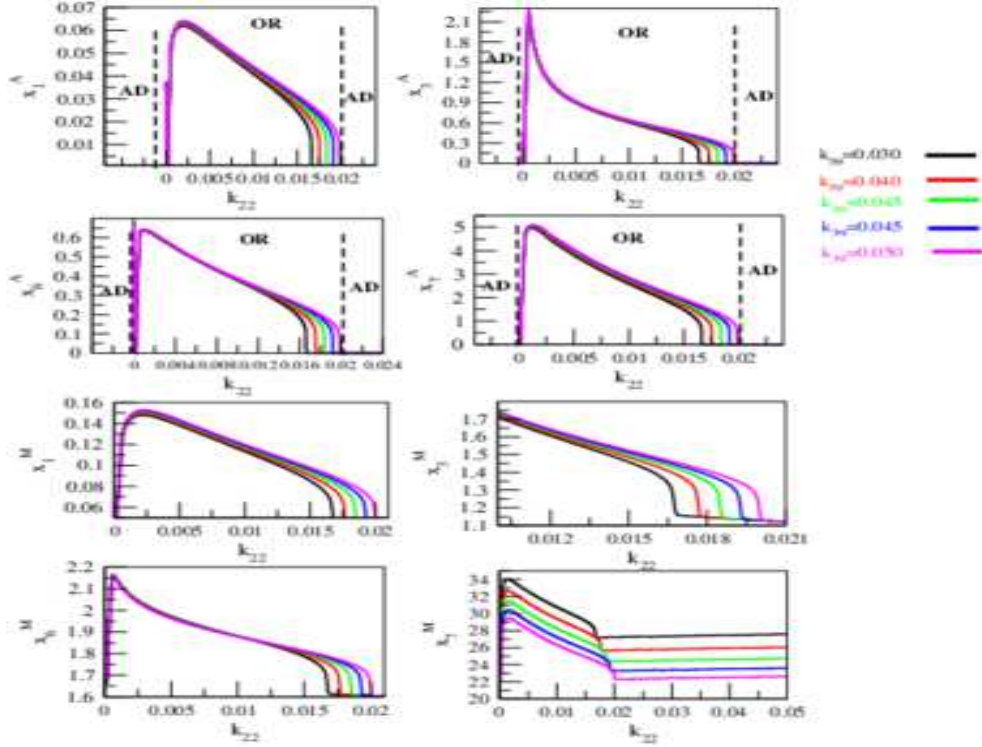


**Figure 6.** Similar plots of  $p53$  ( $x_1$ ),  $\beta$ -catenin ( $x_3$ ),  $Gsk3$  ( $x_6$ ) and  $p53$  ( $x_7$ ) as a function of  $k_{22}$  for the same  $k_{39}$  values as in Figure 5.

### Amplitude death driven by $Gsk3$ and $p53$ interaction

We now study the impact of interaction of  $Gsk3$  and  $p53$  ( $k_{46}$ ) on Wnt and  $p53$  cross talk driven by Nutlin concentration level in the system (Fig. 5). The rate of interaction of  $p53$  and  $Gsk3$  can be modulated by external catalytic action or external stimuli regulating the interaction in the system.

#### Wnt cycle arrest induced by Nutlin

We calculated amplitudes of four molecular species Axin,  $\beta$ -Catenin,  $Gsk3$  and  $Mdm2$  as a function of  $k_{35}$  for five different values of  $k_{46}$  (Fig. 5 upper two rows). The amplitudes of the molecular species for every value of  $k_{42}$  are calculated by averaging the amplitudes within the interval of time [100, 1500] minutes. From the results we observe three different regimes for each value of  $k_{46}$ : first amplitude death (AD) regime (for small  $k_{35}$ ); second finite amplitude or oscillation regime (OR) (for moderate  $k_{35}$ ); and third amplitude death regime again (for large  $k_{35}$ ). The first AD regime may correspond to normal state (stable state) of the system, and second AD regime may correspond to apoptosis (cycle arrest) of the system. Further, we calculated maximum values of molecular species Axin,  $\beta$ -Catenin,  $Gsk3$  and  $p53$  for the corresponding values taken above (Fig. 6 lower two rows of plots). The patterns obtained in these plots are similar to the patterns of the amplitude plots of the corresponding molecular species.

In OR, the amplitude is finite and increases monotonically as a function of  $k_{42}$ , then reaches a maximum amplitude, after which amplitude decreases slowly and then decreases monotonically. This is the regime where the system is in activated or stress condition. It is also to be noted that as  $k_{46}$  increases the amplitude also increases and the range of activated regime also increases. This means that increasing

$k_{46}$  force the system to get activated quickly and protects the system from next stabilized regime (cycle arrest or apoptosis regime). Therefore, even though increase in Nutlin concentration drives the system to apoptosis regime quickly, one can modulate the interaction of  $p53$  and  $Gsk3$  to protect the system from apoptosis upto significant range of Nutlin concentration level, so that the system can repair back from toxic due to excess Nutlin to come back to normal condition.

### **$p53$ cycle arrest induced by Axin**

Now we study the impact of  $p53$  and  $Gsk3$  interaction on the condition of activation of molecular species of both the  $p53$  and Wnt oscillators. We calculated the amplitudes of these molecular species as a function of Axin concentration level in the system ( $k_{22}$ ) (Fig. 6 first two rows) for the same parameter values as we had taken in the case of calculation of amplitudes of these molecular species with the variation of Nutlin concentration in the system. For the same parameter values we also calculated the maxima of these molecular species (Fig. 6 lower two rows).

The change in  $k_{22}$  drives the amplitudes of all the molecular species to different oscillation states (AD, OR, AD) as we have obtain in the case of Wnt cycle arrest by  $k_{42}$  variation. The increase in Axin concentration level in the system forces amplitudes of the molecular species variables to pass the trajectories of first AD (normal condition), then OR (stress condition) and then second AD (cycle arrest condition). However, in this case the amplitudes of the variables do not change much as a function  $k_{22}$ , but significant change in the range of second AD as a function of  $k_{46}$ . The results indicate the Axin induced  $p53$  cycle arrest, however, interaction of  $p53$  and  $Gsk3$  can able to protect the system from apoptosis upto significant range of  $k_{22}$  so that the system can repair back to its normal condition.

### **Steady state solution of the system**

Since the direct and exact analytical solution of the set of coupled nonlinear differential equations (1), we used quasi steady state approximation [51, 52] to obtain approximation solution of the system. Using steady state values of the fast variables using (15), putting back to the ODE of  $x_1(t)$  in equation (16) and taking  $\frac{x_1}{k_{24}+x_1} \sim \frac{1}{1+\frac{k_{24}}{x_1}} \sim \left(1 - \frac{k_{24}}{x_1}\right) \sim 1$  (for large  $x_1$ ) we get the following approximate solutions of  $x_1$ ,

$$x_1(t) \approx \frac{u_1}{u_2} + C_1 e^{-u_2 t} \quad (18)$$

where,  $C_1$  is a constant, and  $u_1, u_2$  are also given by,

$$\begin{aligned} u_1 &= k_{26} \left( k_{22}x_2^* + k_2k_8 - \frac{u_2k_2}{k_1k_{26}} - k_{23} \right) \\ u_2 &= \frac{k_1k_{26}k_{40}x_{13}^*}{\frac{k_{39}}{k_{28}}(k_{41}x_{13}^* - k_{29}x_9^*)} \end{aligned} \quad (19)$$

The equation (18) shows that  $x_1$  becomes constant (steady state) as  $t \rightarrow \infty$ . However,  $x_1$  depends on various other steady state variables as shown in equation (18) and (19).

We then solve ODE of  $x_3(t)$  in equation (16) for  $x_3$ , and the result is given by,

$$x_3(t) \approx \frac{k_3 - k_{14}x_4^*}{k_{13}} + C_2 e^{-k_{13}k_{26}t} \quad (20)$$

where,  $C_2$  is a constant. Here, in this solution, we can get that  $x_3$  stabilizes to a constant value at sufficiently large time limit ( $t \rightarrow \infty$ ).

Now, the approximate solution of  $x_6$  can be obtained by solving ODE of  $x_6$  in equation (16), using equation (18) and (17), as given below,

$$x_6(t) \approx \exp(at - be^{-u_2 t}) \left[ C_3 - \left( \frac{u_3}{u_2} \right) b^{a/u_2} \Gamma \left( -\frac{a}{u_2}, b \right) \right] \quad (21)$$

where,  $C_3$  is a constant. Similarly,  $u_3 = k_2 k_8 k_{26}$ ,  $a = \frac{k_1 k_{26} u_1}{u_2}$  and  $b = \frac{k_1 k_{26} C_1}{u_2}$  are also constants.

The molecular species  $x_{11}$  can be solved directly from equation (16) and using equation (17). The result is given by,

$$x_{11}(t) \approx C_4 e^{-k_{38} t} + \frac{k_{35}}{k_{38}} \quad (22)$$

where,  $C_4$  is a constant. Further, using the differential equation in  $x_7$  in equation (16) and equation (22) along with equation (17), we solve for  $x_7$  given by,

$$\begin{aligned} x_7(t) &\approx \frac{\frac{u_4}{k_{38}} \int \frac{y^{u_5/k_{38} t}}{y - C_4} dy + C_5}{\left[ C_4 + \frac{k_{35}}{k_{38}} e^{k_{38} t} \right]} \\ &\approx \frac{2\pi i \frac{u_4}{k_{38}} C_4^{\frac{u_5}{k_{38}}} + C_5}{\left[ C_4 + \frac{k_{35}}{k_{38}} e^{k_{38} t} \right]} \end{aligned} \quad (23)$$

where,  $u_4 = k_{31} + k_{34} x_{10}^*$ ,  $u_5 = \frac{1}{k_{36}} (k_{33} k_{37} x_{12}^*)$  and  $C_5$  is a constant. Similarly, the variable  $x_8$  can be solved using equations (16), (22) and (17) as follows,

$$\begin{aligned} x_8(t) &\approx \frac{C_6 - \frac{k_{27} x_9^*}{k_{38}} \int y^{-\left(1 + \frac{u_6}{k_{38}}\right)} e^{-\frac{u_7}{k_{38}} y} dy}{e^{-u_6 t + \frac{u_7}{k_{38}} e^{-k_{38} t}}} \\ &\approx \frac{C_6 - \frac{k_{27} x_9^*}{k_{38}} E_1 + \frac{u_7}{k_{38}} \left( \frac{u_7}{k_{38}} \right)}{e^{-u_6 t + \frac{u_7}{k_{38}} e^{-k_{38} t}}} \end{aligned} \quad (24)$$

where,  $u_6 = k_{38} + \frac{k_{35} k_{36}}{k_{38}}$ ,  $u_7 = k_{36} C_1$  and  $C_6$  are constants.  $E$  is the error function.

## Conclusion

The cross talk between  $p53$  and Wnt oscillators can influence each other such that the dynamics one oscillator can regulate the dynamics of the other and vice versa. The concentration level of Nutlin can drive the  $p53$  network module to different oscillating states corresponding to different stress states of the system. This changes in the oscillating states can be well communicated to Wnt network module via  $Gsk3$  and could able to regulate the Wnt functionalities. Further, this changes can well interfere and give impact on the process of somatogenesis of Wnt network module. On the other hand, the available concentration level of Axin in Wnt network module can also influence the dynamics of molecular species variables in Wnt network module at different stress states. Then the information of these changes is well process by the  $p53$  network module via  $Gsk3$  and capture the changes accordingly. This means that the  $p53$  and Wnt network modules can cross talk between them and regulate each other due to changes in each oscillator by processing information between them. However, excess changes in each network module can act as toxic to each module and arrest the cycle of the other, and vice versa.

We then demonstrate that any other changes in the regulation of the network module, may probably by catalytic reaction or external stimuli which alters the rate of the reaction of a particular reaction, can

probably try to protect the system from apoptosis upto certain range of system's condition within which the system can repair back the changes to come back to normal condition. We attempt to numerically demonstrate this phenomena by allowing the change in the rate constant of *p53* and *Gsk3* interaction and clearly give a chance to both the *p53* and Wnt network modules upto certain range of excess concentration levels of Nutlin and Axin to protect themselves from cycle arrest, namely apoptosis. This means that one important role of catalytic reaction and external stimuli (which do not affect the reactions and network but rate of reactions) is to protect the system from apoptosis or system's failure by giving a chance of repair the failure or defect by itself within the system automatically. Therefore, we need to find out various such reactions and stimuli in cellular network in order to control and prevent the cell from cell death, due to cellular breakdown by diseases or other external mechanisms, by regulating these important reactions and stimuli.

## References

1. L Collavin, A Lunardi, G Del Sal. 2010 p53-family proteins and their regulators: hubs and spokes in tumor suppression. *Cell Death and Differentiation* 17, 901911.(doi:10.1038/cdd.2010.35)
2. Oren, M., Damalas, A., Gottlieb, T., Michael, D., Taplick, J., Leal, J.F., Maya, R., Moas, M., Seger, R., Taya, Y., et al. 2002 Regulation of p53: intricate loops and delicate balances. *Biochem Pharmacol* 64, 865-871. (doi:S0006295202011498).
3. Itahana, K., Dimri, G.Campisi, J. 2001 Regulation of cellular senescence by p53. *Eur J Biochem* 268, 2784-2791.(doi: 10.1046/j.1432-1327.2001.02228.x).
4. Vogelstein, B., Lane, D. & Levine, A.J. 2000 Surfing the p53 network. *Nature* 408, 307-310.(doi:10.1038/35042675)
5. Agarwal, M.L., Taylor, W.R., Chernov, M.V., Chernova, O.B., Stark, G.R. 1998 The p53 network. *J Biol Chem* 273, 1-4.(doi: 10.1074/jbc.273.1.1)
6. Purvis, J.E., Karhohs, K.W., Mock, C., Batchelor, E., Loewer, A., Lahav, G. p53 dynamics control cell fate. *Science* 336, 1440-1444. (doi:336/6087/1440)
7. Lowe SW, Cepero E, Evan G. 2004 Intrinsic tumour suppression. *Nature* 432, 307-315.19. (doi:10.1038/nature03098).
8. Momand, J., Wu, H.H., Dasgupta, G. 2000 MDM2-master regulator of the p53 tumor suppressor protein. *Gene* 242, 15-29. (doi:S0378-1119(99)00487-4)
9. Toledo F,Wahl GM. 2006 Regulating the p53 pathway: in vitro hypotheses, in vivo veritas. *Nat Rev Cancer* 6, 909-923.7. (doi:10.1038/nrc2012)
10. Honda R, Tanaka H,Yasuda H. 1997 Oncoprotein MDM2 is a ubiquitin ligase E3 for tumor suppressor p53. *FEBS Lett* 420, 25-27.(doi:S0014-5793(97)01480-4).
11. Kobet E, Zeng X, Zhu Y, Keller D,Lu H. 2000 MDM2 inhibits p300-mediated p53 acetylation and activation by forming a ternary complex with the two proteins. *Proc Natl Acad Sci U S A* 97, 12547-12552.(doi:10.1073/pnas.97.23.12547 97/23/12547).
12. Oliner JD, Kinzler KW, Meltzer PS, George DL, Vogelstein B. 1992 Amplification of a gene encoding a p53-associated protein in human sarcomas. *Nature* 358, 80-83.29.(doi:10.1038/358080a0).
13. Chen, J., Wu, X., Lin, J., Levine, A.J. 1996 mdm-2 inhibits the G1 arrest and apoptosis functions of the p53 tumor suppressor protein. *Mol Cell Biol* 16, 2445-2452.



14. Haupt, Y., Barak, Y., Oren, M. 1996 Cell type-specific inhibition of p53-mediated apoptosis by mdm2. *EMBO J* 15, 1596-1606.
15. Arora, A., Gera, S., Maheshwari, T., Raghav, D., Alam, M.J., Singh, R.K. Agarwal, S.M. The dynamics of stress p53-Mdm2 network regulated by p300 and HDAC1. *PLoS One* 8, e52736. (doi:10.1371/journal.pone.0052736PONE-D-12-06209).
16. Oren, M. 2003 Decision making by p53: life, death and cancer. *Cell Death Differ* 10, 431-442. (doi:10.1038/sj.cdd.44011834401183).
17. Shangary, S., Wang, S. 2009 Small-molecule inhibitors of the MDM2-p53 protein-protein interaction to reactivate p53 function: a novel approach for cancer therapy. *Annu Rev Pharmacol Toxicol* 49, 223-241. (doi:10.1146/annurev.pharmtox.48.113006.094723).
18. Momand, J., Zambetti, G.P., Olson, D.C., George, D., Levine, A.J. 1992 The mdm-2 oncogene product forms a complex with the p53 protein and inhibits p53-mediated transactivation. *Cell* 69, 1237-1245. (doi:0092-8674(92)90644-R).
19. Vassilev LT, Vu BT, Graves B, Carvajal D, Podlaski F, Filipovic Z, Kong N, Kammlott U, Lukacs C, Klein C et al. 2004 In vivo activation of the p53 pathway by small-molecule antagonists of MDM2. *Science* 303, 844-848.(doi:10.1126/science.1092472 1092472).
20. Logan IR, McNeill HV, Cook S, Lu X, Lunec J, Robson CN. 2007 Analysis of the MDM2 antagonist nutlin-3 in human prostate cancer cells. *Prostate* 67, 900-906.(doi:10.1002/pros.20568).
21. Villalonga-Planells R, Coll-Mulet L, Martinez-Soler F, Castano E, Acebes JJ, Gimenez-Bonafe P, Gil J, Tortosa A. 2011 Activation of p53 by nutlin-3a induces apoptosis and cellular senescence in human glioblastoma multiforme. *PLoS One* 6, e18588.(doi:10.1371/journal.pone.0018588).
22. Binder, B.R. 2007 A novel application for murine double minute 2 antagonists: the p53 tumor suppressor network also controls angiogenesis. *Circ Res* 100, 13-14. (doi: 10.1161/01.RES.0000255897.84337.38).
23. Lee SY, Shin SJ, Kim HS. 2013 ERK1/2 activation mediated by the nutlin3-induced mitochondrial translocation of p53. *Int J Oncol* 42, 1027-1035.(doi:10.3892/ijo.2013.1764).
24. Aulehla, A., Agarwal, O. 2008 Oscillating signaling pathways during embryonic development. *Curr Opin Cell Biol* 20, 632-637. (doi:10.1016/j.ceb.2008.09.002).
25. Gibb, S., Zagorska, A., Melton, K., Tenin, G., Vacca, I., Trainor, P., Maroto, M., Dale, J.K. 2009 Interfering with Wnt signalling alters the periodicity of the segmentation clock. *Dev Biol* 330, 21-31.(doi:10.1016/j.ydbio.2009.02.035)
26. Gibb, S., Maroto, M., Dale, J.K. 2010 The segmentation clock mechanism moves up a notch. *Trends Cell Biol* 20, 593-600.(doi: 10.1016/j.tcb.2010.07.001)
27. Goldbeter, A., Pourquie, O. 2008 Modeling the segmentation clock as a network of coupled oscillations in the Notch, Wnt and FGF signaling pathways. *J Theor Biol* 252, 574-585.(doi:10.1016/j.jtbi.2008.01.006).
28. Dequeant, M.L., Glynn, E., Gaudenz, K., Wahl, M., Chen, J., Mushegian, A., Pourquie, O. 2006 A complex oscillating network of signaling genes underlies the mouse segmentation clock. *Science* 314, 1595-1598. (doi:10.1126/science.1133141).

29. Pourquie, O. 2003 The segmentation clock: converting embryonic time into spatial pattern. *Science* 301, 328-330.(DOI: 10.1126/science.1085887).
30. Peng, X., Yang, L., Chang, H., Dai, G., Wang, F., Duan, X., Guo, L., Zhang, Y., Chen, G. Wnt/beta-catenin signaling regulates the proliferation and differentiation of mesenchymal progenitor cells through the p53 pathway. *PLoS One* 9, e97283. (doi:10.1371/journal.pone.0097283).
31. Kim NH, Kim HS, Kim NG, Lee I, Choi HS, Li XY, Kang SE, Cha SY, Ryu JK, Na JM et al. 2011 p53 and microRNA-34 are suppressors of canonical Wnt signaling. *Sci Signal* 4, ra71.(doi:10.1126/scisignal.2001744).
32. Cha YH, Kim NH, Park C, Lee I, Kim HS, Yook JI. 2012 MiRNA-34 intrinsically links p53 tumor suppressor and Wnt signaling. *Cell Cycle* 11, 1273-1281.(doi:10.4161/cc.19618).
33. Tauriello DV, Maurice MM. 2010 The various roles of ubiquitin in Wnt pathway regulation. *Cell Cycle* 9, 3700-3709.(doi:10.4161/cc.9.18.13204).
34. Kim, N.H., Cha, Y.H., Kang, S.E., Lee, Y., Lee, I., Cha, S.Y., Ryu, J.K., Na, J.M., Park, C., Yoon, H.G., et al. 2013 p53 regulates nuclear GSK-3 levels through miR-34-mediated Axin2 suppression in colorectal cancer cells. *Cell Cycle* 12, 1578-1587. (doi:10.4161/cc.24739).
35. Doble BW, Woodgett JR. 2003 GSK-3: tricks of the trade for a multi-tasking kinase. *J Cell Sci* 116, 1175-1186.(doi: 10.1242/jcs.00384)
36. Woodgett JR. 2001 Judging a protein by more than its name: GSK-3. *Sci STKE* 2001, re12.18. (doi:10.1126/stke.2001.100.re12 2001/100/re12).
37. Aberle H, Bauer A, Stappert J, Kispert A, Kemler R. 1997  $\beta$ -catenin is a target for the ubiquitin-proteasome pathway. *EMBO J* 16, 3797-3804.(doi:10.1093/emboj/16.13.3797).
38. Nakamura, T., Hamada, F., Ishidate, T., Anai, K., Kawahara, K., Toyoshima, K., Akiyama, T. 1998 Axin, an inhibitor of the Wnt signalling pathway, interacts with beta-catenin, GSK-3 $\beta$  and APC and reduces the beta-catenin level. *Genes Cells* 3, 395-403.( DOI: 10.1046/j.1365-2443.1998.00198.x)
39. Taelman VF, Dobrowolski R, Plouhinec JL, Fuentealba LC, Vorwald PP, Gumper I, Sabatini DD, De Robertis EM. 2010 Wnt signaling requires sequestration of glycogen synthase kinase 3 inside multivesicular endosomes. *Cell* 143, 1136-1148.(doi:S0092-8674(10)01356-5. 10.1016/j.cell.2010.11.034).
40. Logan IR, McNeill HV, Cook S, Lu X, Lunec J, Robson CN. 2007 Analysis of the MDM2 antagonist nutlin-3 in human prostate cancer cells. *Prostate* 67, 900-906.(doi:10.1002/pros.20568).
41. Jensen, P.B., Pedersen, L., Krishna, S., Jensen, M.H. A Wnt oscillator model for somitogenesis. *Biophys J* 98, 943-950. (doi:10.1016/j.bpj.2009.11.039).
42. Clevers H. 2006 Wnt/ $\beta$ -catenin signaling in development and disease. *Cell* 127, 469-480. (doi:10.1016/j.cell.2006.10.018).
43. Huelsken J, Behrens J. 2002 The Wnt signalling pathway. *J Cell Sci* 115, 3977-3978.(doi: 10.1242/jcs.00089)
44. Wang HY, Huang YX, Qi YF, Zhang Y, Bao YL, Sun LG, Zheng LH, Zhang YW, Ma ZQ, Li YX. 2013 Mathematical models for the Notch and Wnt signaling pathways and the crosstalk between them during somitogenesis. *Theor Biol Med Model* 10, 27. (doi:10.1186/1742-4682-10-27).
45. Proctor CJ, Gray DA. 2008 Explaining oscillations and variability in the p53-Mdm2 system. *BMC Syst Biol* 2, 75.(doi:10.1186/1752-0509-2-75).

46. Devi, G.R., Alam, M.J., Singh, R.K. Synchronization in stress p53 network. *Math Med Biol.* (doi:10.1093/imammb/dqv002).
47. Alam, M.J., Devi, G.R., Ravins, Ishrat, R., Agarwal, S.M., Singh, R.K. Switching p53 states by calcium: dynamics and interaction of stress systems. *Mol Biosyst* 9, 508-521. (doi:10.1039/c3mb25277a).
48. Proctor CJ, Gray DA. 2010 GSK3 and p53 - is there a link in Alzheimer's disease? *Mol Neurodegener* 5,7. (doi:10.1186/1750-1326-5-7).
49. Chickarmane V, Nadim A, Ray A, Sauro HM. 2005 A p53 Oscillator Model of DNA Break Repair Control. arXiv preprint q-bio/051002.
50. Lahav G, Rosenfeld N, Sigal A, Geva-Zatorsky N, Levine AJ, Elowitz MB, Alon U. 2004 Dynamics of the p53-Mdm2 feedback loop in individual cells. *Nat Genet* 36, 147-150.(doi:10.1038/ng1293ng1293).
51. J.D. Murray. 2003 *Mathematical Biology I and II*. Springer-Verlag 3rd Edition.
52. M. Schauer and R. Heinrich. 1983 Quasi-steady state approximation in the Mathematical modeling of Biochemical reaction networks. *Math. Biosc.* 65, 155-170.
53. MG Pedersen, AM Bersani and E Bersani. Quasi steady-state approximations in complex intracellular signal transduction networks-a word of caution. *J. Math. Chem.* 43, 1318 (2007).
54. Gu W,Roeder RG. 1997 Activation of p53 sequence-specific DNA binding by acetylation of the p53 C-terminal domain. *Cell* 90, 595-606.(doi:10.1016/S0092-8674(00)80521-8)

Table 1-List of molecular species and their intial concentration

S.No.	Species Name	Description	Notation	Intial Concentration(nM)
1.	<i>Axin2</i>	Intial Concentration <i>Axin2</i> protein	$x_1$	10.0
2.	<i>Axin2</i> _mRNA	Intial Concentration <i>Axin2</i> _mRNA	$x_2$	0.1
3.	$\beta$ -catenin	UnPhosphorylated $\beta$ -catenin	$x_3$	0.1
4.	$\beta$ -catenin_p	Phosphorylated $\beta$ -catenin	$x_4$	0.001
5.	$\beta$ -catenin_n	Nuclear $\beta$ -catenin	$x_5$	0.1
6.	<i>Gsk3</i>	Gsk3 protien	$x_6$	5.0
7.	<i>p53</i>	unbound <i>p53</i> protein	$x_7$	0.022
8.	<i>MDM2</i>	Unbound <i>MDM2</i> protien	$x_8$	0.035
9.	<i>MDM2</i> _mRNA	<i>MDM2</i> Messsenger mRNA	$x_9$	0.01
10.	<i>p53_MDM2</i>	<i>MDM2</i> and <i>p53</i> complex	$x_{10}$	0.01
11.	Nutlin	Unbound Nutlin	$x_{11}$	0.0425
12.	Nutlin_ <i>MDM2</i>	Nutlin <i>MDM2</i> complex	$x_{12}$	0.01
13.	<i>p53_Gsk3</i>	<i>p53</i> and <i>Gsk3</i> complex	$x_{13}$	0.01

Table 2 List of parameter

S.No.	Notation	Description	Values	Reference
1.	$K_1$	Rate constant for binding of <i>Gsk3</i> to <i>Axin2</i>	$0.23nMmin^{-1}$	[27]
2.	$K_2$	Rate constant for dissociation of <i>Gsk3_Axin2</i>	$0.1min^{-1}$	[27]
3.	$K_3$	Rate of $\beta$ -catenin synthesis	$0.087nMmin^{-1}$	[27]
4.	$K_4$	Rate of $\beta$ -catenin entry into the nucleus	$0.7min^{-1}$	[27]
5.	$K_5$	Rate of $\beta$ -catenin exit from the nucleus	$1.5min^{-1}$	[27]
6.	$K_6$	Rate of phosphorylation of $\beta$ -catenin by the <i>Gsk3</i>	$5.08nMmin^{-1}$	[27]
7.	$K_7$	Concentration of Dishevelled(Dsh)protein	$2.0nM$	[27]
8.	$K_8$	Total <i>Gsk3</i> Concentration	$3.0nM$	[27]
9.	$K_9$	Rate of inhibition by Dsh for $\beta$ -catenin_p by the <i>Axin2_Gsk3</i> complex	$0.5nM$	[27]
10.	$K_{10}$	Rate constant for $\beta$ -catenin_p by the <i>Axin2_Gsk3</i> complex	$0.28nM$	[27]
11.	$K_{11}$	Rate constant of dephosphorylation of $\beta$ -catenin	$1.0nMmin^{-1}$	[27]
12.	$K_{12}$	Maximum rate constant for $\beta$ -catenin phosphora-tion	$0.003nM$	[27]
13.	$K_{13}$	Rate constant for degradation of unphosphorylated $\beta$ -catenin	0	[27]
14.	$K_{14}$	Rate constant for degradation of phosphorylated $\beta$ -catenin	$7.062min^{-1}$	[27]
15.	$K_{15}$	Rate of transcription of the <i>Axin2</i> gene	$0.06nMmin^{-1}$	[27]
16.	$K_{16}$	Rate of transcription of the <i>Axin2</i> gene induced by nuclear $\beta$ -catenin	$1.64nMmin^{-1}$	[27]
17.	$K_{17}$	Rate for induction by nuclear $\beta$ -catenin of <i>Axin2</i> gene trascription	$0.7nM$	[27]
18.	$K_{18}$	Maximum Rate of degradation of <i>Axin2</i> _mRNA	$0.8nMmin^{-1}$	[27]
19.	$K_{19}$	Rate constant for degradation of <i>Axin2</i> _mRNA	$0.48nM$	[27]
20.	$K_{20}$	Rate of transcription of <i>Axin2</i> gene induced by transcription factor	$0.5nMmin^{-1}$	[27]
21.	$K_{21}$	rate for induction by transcription factor of <i>Axin2</i> gene transcription	$0.05nM$	[27]
22.	$K_{22}$	Rate of synthesis of <i>Axin2</i> protein	$0.02min^{-1}$	[27]
23.	$K_{23}$	Maximum rate of degradtion of <i>Axin2</i> protein	$0.6nMmin^{-1}$	[27]
24.	$K_{24}$	Michaelis rate for degradtion of <i>Axin2</i> protein	$0.63nM$	[27]
25.	$K_{25}$	Hill coefficients	2.0	[27]
26.	$k_{26}$	Scaling factor for Wnt oscillator	1.5	[27]
27.	$k_{27}$	<i>MDM2</i> synthesis	$0.297min^{-1}$	[45]
28.	$k_{28}$	<i>MDM2</i> transcripton	$0.006min^{-1}$	[45]
29.	$k_{29}$	<i>MDM2<sub>m</sub>RNA</i> degradation	$0.006min^{-1}$	[45]
30.	$k_{30}$	<i>MDM2</i> degradation	$0.2598min^{-1}$	[45]
31.	$k_{31}$	<i>p53</i> synthesis	$4.68min^{-1}$	[45]
32.	$k_{32}$	<i>p53</i> degradation	$0.0495min^{-1}$	[45]
33.	$k_{33}$	<i>p53_MDM2</i> binding	$0.693min^{-1}$	[45]



Table 2 Continue...

S.No.	Notation	Description	Values	Reference
34.	$k_{34}$	$p53\_MDM2$ dissociation	$0.00693min^{-1}$	[45]
35.	$k_{35}$	Nutilin formation	$0.001min^{-1}$	Estimated
36.	$k_{36}$	Nutilin $MDM2$ formation	$0.012min^{-1}$	Estimated
37.	$k_{37}$	Nutilin $MDM2$ degradation	$0.03min^{-1}$	Estimated
38.	$k_{38}$	Nutilin degaradation	$0.06min^{-1}$	Estimated
39.	$k_{39}$	$p53\_Gsk3$ complex formation	$0.04min^{-1}$	[48]
40.	$k_{40}$	$p53\_Gsk3$ complex degradation	$0.12min^{-1}$	[48]
41.	$k_{41}$	$MDM2\_mRNA$ synthesis	$0.042min^{-1}$	[48]